Advance and retreat of the marine-terminating Irish Sea Ice Stream into the Celtic Sea during the Last Glacial: Timing and maximum extent

Scourse, James; Saher, Margot; Van Landeghem, Katrien; Lockhart, Edward; Purcell, Catriona; Callard, Sarah Louise; Roseby, Zoe; Allison, Ben; Piekowski, Anna; Ó Cofaigh, Colm; Praeg, Daniel; Ward, Sophie; Chiverrell, R.C.; Moreton, Steven; Fabel, Derek; Clark, Chris

Marine Geology

DOI:
10.1016/j.margeo.2019.03.003

Published: 01/06/2019

Publisher's PDF, also known as Version of record

Marine Geology 412 (2019) 53–68

Contents lists available at ScienceDirect

Marine Geology

journal homepage: www.elsevier.com/locate/margo

Advance and retreat of the marine-terminating Irish Sea Ice Stream into the Celtic Sea during the Last Glacial: Timing and maximum extent

James Scourse[a,*], Margot Saher[b], Katrien J.J. Van Landeghem[b,c,d], Edward Lockhart[b], Catriona Purcell[b], Louise Callard[f], Zoe Roseby[b,c,d], Ben Allinson[b], Anna J. Pieńkowski[e], Colm O'Cofaigh[f], Daniel Praeg[g,h], Sophie Ward[b], Richard Chiverrell[i], Steve Moreton[j], Derek Fabel[k], Chris D. Clark[l]

[a] College of Life and Environmental Sciences, University of Exeter, Penryn, Cornwall TR10 9EZ, UK
[b] School of Ocean Sciences, Bangor University, Menai Bridge, Anglesey LL59 5AB, UK
[c] Ocean and Earth Sciences, University of Southampton, Southampton SO14 3ZH, UK
[d] National Oceanography Centre, University of Southampton Waterfront Campus, Southampton SO14 3ZH, UK
[e] University Centre in Svalbard (UNIS), Department of Arctic Geology, N-9171 Longyearbyen, Svalbard, Norway
[f] Department of Geography, Durham University, Durham, UK
[g] OGS (Istituto Nazionale di Oceanografia e di Geofisica Sperimentale), Borgo Grotta Gigante, 34010 Trieste, Italy
[h] Laboratório de Geologia Marinha, Universidade Federal Fluminense, Brazil
[i] School of Environmental Sciences, University of Liverpool, Liverpool, UK
[j] NERC Radiocarbon Laboratory, East Kilbride, UK
[k] Scottish Universities Environmental Research Centre, East Kilbride, UK
[l] Department of Geography, University of Sheffield, Sheffield, UK

ARTICLE INFO

Editor: Michele Rebesco

Keywords:
Shelf (morphology and stratigraphy)
Glacial sediments
Geophysics (seismic)
Quaternary stratigraphy
Micropaleontology (forams)
Europe

ABSTRACT

The dynamics of the British-Irish Ice Sheet (BIIS) during the Last Glacial were conditioned by marine-based ice streams, the largest of which by far was the Irish Sea Ice Stream (ISIS) which drained southwest across the Celtic shelf. The maximum extent and timing of the ISIS have been constrained by onshore evidence from the UK and Ireland, and by glacigenic sediments encountered in a small suite of vibrocores from the UK-Irish continental shelf, from which a single radiocarbon date is available. These data have long supported ice advance to at least the mid-shelf, while recent results suggest the ISIS may have extended 150 km farther seaward to the shelf edge. The glacigenic sequences have not been placed within a secure seismic-stratigraphic context and the relationship between glaciation and the linear sediment megaridges observed on the outer shelf of the Celtic Sea has remained uncertain. Here we report results of sedimentological, geochemical, geochronological and micropalaeontological analyses combined with a seismic-stratigraphic investigation of the glacigenic sequences of the Celtic Sea with the aims of establishing maximum extent, depositional context, timing and retreat chronology of ISIS. Eight lithofacies packages are identified, six of which correlate with seismic facies. Lithofacies LF1 and LF2 correlate to a seafloor seismic facies (SF1) that we interpret to record the postglacial and Holocene transgressive flooding of the shelf. Lithofacies LF10 (till), LF3, LF4 and LF8 (glacimarine) correlate to different seismic facies that we interpret to be of glacigenic origin based on sedimentological, geotechnical and micropalaeontological evidence, and their distribution, supported by geochemical evidence from lithofacies LF8 and LF10 indicate extension of ISIS as far as the Celtic Sea shelf break. New radiocarbon ages on calcareous micro- and macrofauna constrain this advance to be between 24 and 27 cal ka BP, consistent with pre-existing geochronological constraints. Glacimarine lithofacies LF8 is in places glacitectonically contorted and deformed, indicating ice readvance, but the nature and timing of this readvance is unclear. Retreat out of the Celtic Sea was initially rapid and may have been triggered by high relative sea-levels driven by significant glacio-isostatic depression, consistent with greater ice loads over Britain and Ireland than previously considered.

* Corresponding author.
E-mail address: j.scourse@exeter.ac.uk (J. Scourse).

https://doi.org/10.1016/j.margeo.2019.03.003
Received 1 August 2018; Received in revised form 8 February 2019; Accepted 13 March 2019
Available online 16 March 2019

1. Introduction

There is currently significant concern over the dynamic instability of the marine-based sectors of the West Antarctic Ice Sheet, the rapid deglaciation or collapse of which would have global implications in terms of sea-level change and climate via perturbation to deep ocean circulation (Joughin and Alley, 2011; Rignot et al., 2014). It is therefore important to understand the dynamics of marine-based ice sheets, and the ice streams that drain their accumulation areas, but modelling of these systems is hindered by a lack of observations of the style and deglacial dynamics of former marine-based ice sheets. An alternative approach is to reconstruct in detail the deglacial dynamics of former deglaciating or collapsing marine-based ice sheets and to use these data as a template for ice sheet model development (Stokes et al., 2015).

The last British-Irish Ice Sheet (BIIS) at its maximum extent incorporated significant sectors that were marine-terminating and marine-based (Clark et al., 2012, 2018). The recognition that the BIIS can be used as a basis for understanding rates and processes involved in marine-based ice sheet deglaciation, in which some of the significant drivers of collapse/retreat (atmospheric climate, oceanic climate, relative sea-level change, tidal change, bed slope, trough geometry, internal glaciology; Schoof, 2007; Jamieson et al., 2012) can be independently identified (Small et al., 2018), is the motivation for an ongoing major community research effort, the BRITICE-CHRONO project. This project aims to reconstruct in detail the retreat dynamics of all the significant ice streams and outlet systems of the BIIS from the Last Glacial Maximum (LGM). BRITICE-CHRONO is also using this reconstruction as an input to modelling the deglaciating BIIS and in doing so generically improving numerical model simulations of marine-based ice sheet collapse.

The Irish Sea Ice Stream (ISIS) was by far the largest ice stream to drain the former BIIS (Roberts et al., 2007). With catchment zones in southern Scotland, northern England, Ireland and Wales, the main axis of ISIS flowed from north to south through the Irish Sea Basin (Fig. 1). Glacial landform assemblages linked to legacy onshore geochronological data have been used as the basis for a Bayesian analysis of the advance and retreat stages of the last ISIS (Chiverrell et al., 2013) in which mapped glacigenic landform-sediment associations e.g. morainal banks, provide the *prior* chronological sequence for the analysis. The results of this reconstruction indicate ISIS extension to a marine-terminating limit across the Celtic Sea, with a defined ice limit on the northern Isles of Scilly, at 24 ka (Fig. 1). This timing coincides with independently-dated ice-rafted detritus (IRD) flux from ISIS to the adjacent continental margin (Scourse et al., 2009a; Haapaniemi et al., 2010). The ISIS then retreated rapidly northwards to an oscillating margin that remained in the vicinity of St George's Channel (Small et al., 2018) (Fig. 1), before further receding to another quasi-stable position adjacent to the Llŷn Peninsula (Smedley et al., 2017a) before the final retreat phase into the northern Irish Sea (Chiverrell et al., 2018).

The maximum extension and the timing of the ISIS advance into the Celtic Sea, corresponding to the most southerly extent of the BIIS, are questions of current debate and the focus of this paper. The Celtic Sea extends from St George's Channel in the northeast to the continental shelf break some 200–250 km to the southwest of Ireland and the Isles of Scilly and to the west of Brittany (Fig. 1). Apart from the Celtic Deep, a glacially-excavated and tectonically-controlled bathymetric trough in the axis immediately to the south of St George's Channel extending to depths > 130 m (Furze et al., 2014), the average depth of the northern Celtic shelf is around 100 m. The mean depth of the shelf deepens towards the shelf break at an elevation of ~200 m. The mid and outer Celtic shelf is characterised by a field of megascale linear sediment ridges, which extend over a ~65,000 km^2 area of the Irish, UK and French sectors (Fig. 1). The ridge field overlies offlapping Mesozoic to Cenozoic sequences that constitute the bulk of the shelf (Pantin and Evans, 1984).These features are some of the largest on Earth (Scourse et al., 2009b) and have been previously interpreted as "linear tidal sand ridges" (LTSR), their origin attributed to penecontemporaneous tidal reworking of deglacial ISIS sediments and the shelfal fan accumulations of the Fleuve Manche (Channel River) during early deglaciation (Scourse et al., 2009b). Alternatively, it has been considered that the ridges might be of glacial origin (Belderson et al., 1986; Praeg et al., 2015; Lockhart et al., 2018). The ridge axes are oriented broadly southwest to northeast and terminate landwards to the north and northeast along the 130 m isobath to the southwest of the Isles of Scilly (Fig. 1). The largest ridges, such as the Great Sole and Cockburn banks (Fig. 1), are up to 200 km in length, 55 m high and 15 km wide, with a ridge-to-ridge wavelength of some 20 km (Belderson et al., 1986; Scourse et al., 2009b). Vibrocores recovered by the British Geological Survey in the 1970's and 1980's across the Celtic Sea penetrated, sporadically, thin patches of glacigenic sediments interpreted, on the basis of the position fixing technology available at the time, to be at or close to seabed between, or on the flanks of, the ridges (Pantin and Evans, 1984). In addition, seafloor samples acquired across the Irish-UK shelf reveal gravel to boulder size both between and on the ridges, which together with the core data was suggested to represent a mantle of ice-rafted debris (Pantin and Evans, 1984; Scourse et al., 1991).

Analysis of the glacigenic sediments at the base of the vibrocores (Scourse et al., 1990) showed that they consisted of either overconsolidated, dense, clast-rich diamicton interpreted as subglacial till (Melville Till) or laminated clay-rich silts (Melville Laminated Clay) containing a rich glacimarine microfauna (Ostracoda; benthic foraminifera) (Scourse et al., 1990, 1991). In only one vibrocore (BGS 49/−09/44), recovered from the extreme northern limit of the ridge field (Fig. 1), was the Melville Till observed to be directly overlain by the Melville Laminated Clay (Scourse et al., 1990; Scourse and Furze, 2001). In addition, two cores from the shelf edge encountered clast-rich diamictons, suggested to record iceberg turbates (Scourse et al., 1990). Though no direct dating of the glacigenic sediments was available, Scourse (1991) and Scourse et al., (1990) correlated the Melville Till with the onshore Scilly Till, constrained by conventional radiocarbon and early experimental thermoluminescence and optically stimulated luminescence (OSL) ages to the Last Glacial. Subsequent dating efforts onshore on Scilly (e.g. McCarroll et al., 2010), including the recent BRITICE-CHRONO geochronology (Smedley et al., 2017b), have confirmed the Late Devensian age for the Scilly Till. In correlating, on the basis of lithostratigraphy, the offshore glacigenic sequences with the Scilly Till, Scourse et al. (1990) and Scourse and Furze (2001) interpreted that the advance of ice into the Celtic Sea as a piedmont lobe south of St George's Channel had been a short-lived, surge-type, event over deformable marine substrate. The Melville Till facies was found to be distributed in the northern part of the central Celtic Sea and the Melville Laminated Clay in the southern central Celtic Sea with the boundary between these at ~ 135 mbsl (metres below sea level). Scourse et al. (1990) interpreted this as a palaeo-grounding line but, as pointed out by Sejrup et al. (2005), this has to be regarded as a minimum grounding line position since the southern glacimarine sequences were not penetrated to base by any of the vibrocores.

Praeg et al. (2015) reported the recovery of glacigenic sediments from the flank of outer Cockburn Bank 20 km from the shelf break within the Irish sector. Three vibrocores penetrated up to 0.8 m of seafloor sands to encounter up to 0.4 m of stiff stratified diamict and sticky bedded muddy sands, respectively interpreted as overconsolidated subglacial deposits and glacimarine muds similar to the Melville Laminated Clay. The glacimarine muds contained a single Arctic bivalve mollusc, *Macoma* cf. *moesta*, from which a marine reservoir-corrected radiocarbon determination of 24,265 ± 195 cal yr BP was obtained. This age is significant in that; 1) it constitutes the first direct dating of any of the Celtic Sea glacigenic sequences, and 2) it is consistent with the timing of maximum advance across the Celtic shelf suggested by the Bayesian analysis of onshore data (Chiverrell et al., 2013). The association of the finely-bedded glacimarine sediment with

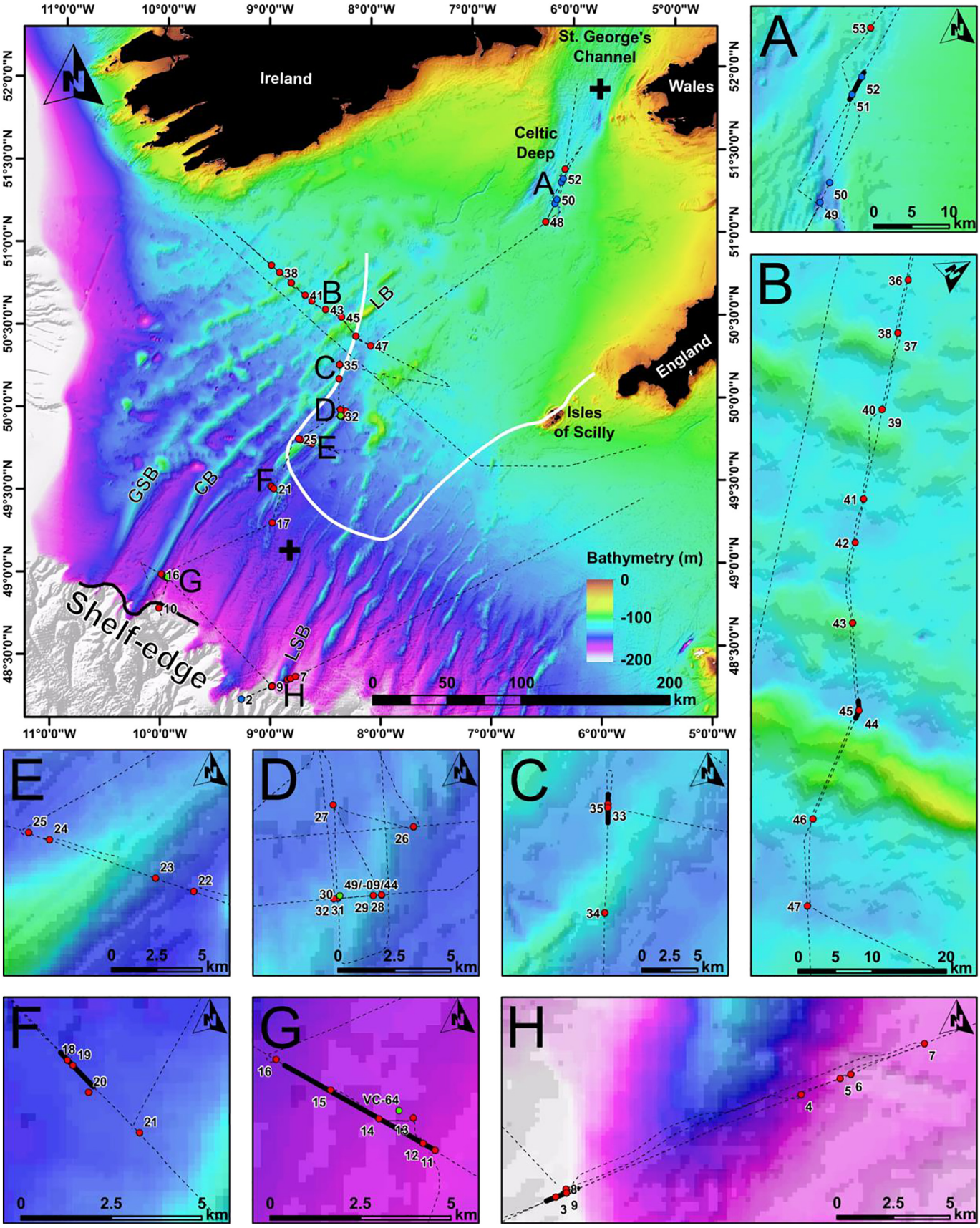

Fig. 1. Bathymetry of the Celtic Sea shelf showing the mid-shelf ice limit at ~135 m OD (white; Scourse et al., 1990) and the shelf-edge limit (black; Praeg et al., 2015). Vibro- (red) and pistoncore (blue) locations with other cores (green) are shown on tracklines (dotted) with insets showing seismic line locations (black). LB: Labadie Bank, CB: Cockburn Bank, LSB: Little Sole Bank, GSB: Great Sole Bank. Black crosses denote RSL simulation locations in Fig. 10. (For interpretation of the references to colour in this figure legend, the reader is referred to the web version of this article.)

overconsolidated stratified diamicts provided a basis to argue against an origin of these sediments as iceberg turbates, as proposed for diamict previously acquired at a nearby site (Scourse et al., 1990), and to propose instead that ISIS extended as far as the shelf break.

This proposal leaves several significant issues unresolved in the Celtic Sea sector of ISIS. The maximum extent of grounded ice is currently based on the interpretation of a glacigenic sequence at the shelf break from which a single radiocarbon age is available whose lithological/geochemical affinity has yet to be linked to an ISIS provenance; although sedimentological arguments against iceberg turbation were offered by Praeg et al. (2015), it remains possible that this shelf edge sequence might alternatively be interpreted as iceberg turbate (cf. Scourse et al. (1990)). The timing of the maximum advance has been well established on Scilly (Smedley et al., 2017b) and in southern (Ó Cofaigh and Evans, 2007; Ó Cofaigh et al., 2012) and eastern Ireland (Small et al., 2018), but offshore the chronology rests on lithostratigraphic correlation (Scourse et al., 1990) and the single radiocarbon determination (Praeg et al., 2015). The glacigenic sequences have yet to be placed within a secure seismic-stratigraphic context, and their stratigraphic relationship to the linear sediment ridges has yet to be established. Moreover, the co-occurrence of fine-grained glacimarine sediments with linear sediment ridges attributed to high energy tidal conditions remains problematic (Ward et al., 2016). Accordingly, in 2014 a BRITICE-CHRONO cruise on the RRS *James Cook* undertook a systematic campaign of sediment sampling (vibrocore, piston core) supported by high frequency seismic reflection profiling in the Celtic Sea in order to establish:

1. Establish the litho- and seismic-stratigraphic context of glacigenic sequences across the Celtic shelf.
2. Test the proposal for the maximum extent of the ISIS across the Celtic shelf.
3. Constrain the timing of the advance and subsequent retreat in relation to the geochronology of terrestrially exposed sequences established onshore by BRITICE-CHRONO in west Wales, southern and eastern Ireland.

This paper presents the data arising from this cruise relating to the distribution of glacigenic sequences across the Celtic shelf, their depositional context and interpretation, and the timing of the ISIS advance across, and retreat from, the shelf. The question of the genetic relationship between this ice advance and the linear sediment ridges is addressed in Lockhart et al. (2018).

2. Materials and methods

2.1. Acoustic data and sediment core acquisition

All cores used in this study (Table 1) were recovered by the RRS *James Cook* during the first part (July 20–27) of cruise JC106 (July 17–August 242,014; cruise track shown on Fig. 1). Coring equipment comprised a British Geological Survey 6 m vibrocorer (VC) and UK National Oceanography Centre 10 m piston corer (PC). A Sonardyne Ranger USBL system provided underwater positioning during coring operations.

To document seafloor morphology in water deeper than 100 m, a hull-mounted 12 kHz Kongsberg Simrad EM120 multibeam system was used, whilst in water shallower than 100 m a drop keel mounted 70–100 kHz EM710 system was employed. In the Celtic Sea both systems collected data simultaneously to maximise data quality, resolution and coverage. Both Applanix POS-MV and Seapath200 acted as the secondary and primary positioning and motion sensor system. Both systems interfaced with a CNAV3050 providing Digital Geographic Position System (DGPS) corrections.

A Kongsberg SBP120 profiler was used to acquire just over 2000 km of sub-bottom seismic reflection profiles across the shelf (Fig. 1). The hull-mounted system uses a transducer with a frequency sweep range of 2.5–7 kHz installed as part of the EM120 wideband receiver array. A smaller beamwidth than a conventional sub-bottom profiler results in improved penetration and a higher angular resolution. The nominal depth resolution is 0.3 ms, although data quality was affected by seabed ringing as well as sea conditions.

Table 1
Locations and water depths of cores used in this study.

Core	Coordinates	Water depth (m)
3VC	48° 19.442′N 8° 59.437′W	211
14VC	48° 59.521′N 9° 58.969′W	168
15VC	48° 59.967′N 10° 0.215′W	165
18VC	49° 32.421′N 8° 59.625′W	146
19VC	49° 32.343′N 8° 59.502′W	145
33VC	50° 16.458′N 8° 20.713′W	132
35VC	50° 16.458′N 8° 20.713′W	130
44VC	50° 33.621′N 8° 19.304′W	125
45VC	50° 33.612′N 8° 19.303′W	125
51PC	51° 20.742′N 6° 11.091′W	116
52PC	51° 21.976′N 6° 09.910′W	116
2PC	48° 14.832′N 9° 15.814′W	459
4VC	48° 21.886′N 8° 50.638′W	169
5VC	48° 22.263′N 8° 49.234′W	179
6VC	48° 22.363′N 8° 48.855′W	182
7VC	48° 23.096′N 8° 46.212′W	175
8VC	48° 19.632′N 8° 59.067′W	198
9VC	48° 19.539′N 8° 59.047′W	197
10VC	48° 47.661′N 10° 1.333′W	206
11VC	48° 58.644′N 9° 56.584′W	172
12VC	48° 58.744′N 9° 56.853′W	170
13VC	48° 59.122′N 9° 57.089′W	168
16VC	48° 59.967′N 10° 0.215′W	160
17VC	49° 18.938′N 8° 58.938′W	146
20VC	49° 31.941′N 8° 59.141′W	143
21VC	49° 31.338′N 8° 57.974′W	137
22VC	49° 47.693′N 8° 36.405′W	142
23VC	49° 48.093′N 8° 38.156′W	122
24VC	49° 49.252′N 8° 43.04′W	125
25VC	49° 49.473′N 8° 44.011′W	129
26VC	49° 59.435′N 8° 17.495′W	131
27VC	49° 59.971′N 8° 20.461′W	134
28VC	49° 57.812′N 8° 18.699′W	125
29VC	49° 57.798′N 8° 19.005′W	122
30VC	49° 57.738′N 8° 20.325′W	124
31VC	49° 57.746′N 8° 20.332′W	125
32VC	49° 57.729′N 8° 20.464′W	125
34VC	50° 11.167′N 8° 21.027′W	118
36VC	50° 52.587′N 8° 59.261′W	116
37VC	50° 49.996′N 8° 54.576′W	119
38VC	50° 49.989′N 8° 54.563′W	120
39VC	50° 46.187′N 8° 47.865′W	119
40VC	50° 46.187′N 8° 47.854′W	119
42VC	50° 39.584′N 8° 36.155′W	123
43VC	50° 36.454′N 8° 28.356′W	99
46VC	50° 26.67′N 8° 11.286′W	121
47VC	50° 23.086′N 8° 3.031′W	134
48VC	51° 6.588′N 6° 20.989′W	110
49PC	51° 13.093′N 6° 15.231′W	133
50PC	51° 14.502′N 6° 14.057′W	128

2.2. Core processing

Cores were cut into sections, split and visually described on board. Lithofacies packages were defined on the basis of texture, colour, clast-content and geotechnical attributes. The correlation of the lithofacies and seismicfacies is described in Lockhart et al. (2018) and summarised in Table 2. A hand-held shear vane was used on exposed core sections to determine undrained shear strength. Any obvious materials for radiocarbon dating were carefully removed from the sediment, cleaned with distilled water and stored for later analysis. Post-cruise selected core sections were X-radiographed in order to reveal further dating targets and to aid sedimentological interpretation.

Table 2
Descriptions of lithofacies and their correlation with other stratigraphic units. See Lockhart et al. (2018) for seismic facies descriptions.

Lithofacies	Lithofacies description	Correlative seismic-facies	Correlative BGS Unit (Lockhart et al., 2018)	Depositional interpretation
LF1	Coarse to medium shelly sands, mostly massive (Sm), occasionally stratified (Sl), fining upwards into massive, soft, greenish-grey muds (Fm)	SF1 (Figs. 4, 5, 6, 7)	Layer A	Post-glacial transgressive (late)
LF1a	Clast-supported muddy shell fragment layer (Gm)	SF1 (Fig. 7)	Layer B	Post-glacial transgressive (early)
LF2	Clast-supported, sometimes shelly, sub-rounded to rounded gravel with coarse to medium sand matrix (Gm)	SF1 (Figs. 4, 5, 6, 7)	Layer B	Post-glacial transgressive (early)
LF3	Soft silty clay unit with fine sand laminations (Fl)	SF2 (Fig. 7)		Glacimarine
LF4	Soft massive silty clay (Fm)	SF3 (Fig. 7)		Glacimarine
LF8	This package contains a number of individual lithofacies including massive fine to medium sands (Sm) in many places laminated (Sl) and/or contorted and deformed (Sd) containing sporadic bivalves or bivalve fragments and dropstones (Sm(d)/Sl(d)/Sd(d)), to massive muds (Fm) and laminated (Fl) and muds with fine sand lenses (Fp), often deformed (Fd). This package is often, though not always, characterised by high shear strengths (between 100 and 200 kPa), especially where the facies are deformed (Fd)	SF6, SF7 (Figs. 3, 4, 5), SF 5 (Fig. 6)	Upper Little Sole Formation	Glacimarine (subglacially reworked)
LF9	Massive fining upward coarse to fine shelly sands (Sm)	SF5 (Fig. 6)	Upper Little Sole Formation	Glacimarine
LF10	A matrix-supported diamicton (Dmm) with high shear strength (between 100 and 200 kPa)	Unknown (Fig. 2)		Subglacial

Selected lithofacies packages (LF8 and LF10) were analysed using X-ray fluorescence (XRF) in order to determine elemental geochemistry. An Olympus DELTA XRF gun was used to collect high resolution major element geochemical records at the University of Liverpool. The Olympus DELTA is an energy dispersive XRF gun and was mounted onto a GEOTEK core scanner. The split cores were analysed using a 4-watt rhodium X-ray tube and a thermoelectrically cooled large area Si drift detector. Cores were scanned at 0.5 cm resolution in soil mode (15, 40, 40 (filtered) kV beam conditions) each beam for 20 s. Data output from the Olympus Delta is in elemental concentrations based on internal calibrations from raw X-ray spectra. A SPECTRO XEPOS energy dispersive XRF spectrometer was used to measure the dry mass composition of sediment subsamples from the scanned cores. These subsamples were weighed, freeze-dried and re-weighed to measure water content and were then homogenised using a pestle and mortar. The instrument emits a combined binary Pd and Co excitation radiation and has a high resolution low spectral interference silicon drift detector. Each sample was measured for 600 s. The wet scan XRF data were corrected to dry mass concentrations by simple regression using the dry sediment elemental concentrations data from the subsamples (Boyle et al., 2015). The corrected data for each core were then averaged over 2.5 cm core thickness. Principal component analysis (PCA) was performed to characterise the elemental assemblages of the cores. The analyses were performed using the RStudio software programme. All parameters were standardised in R before the PCA.

The intended sampling strategy for radiocarbon analysis was to sample articulated filter feeding bivalves in life position just above the deglacial contact. However, few of the cores in the Celtic Sea contained a deglacial contact, and no cores contained articulated filter feeding bivalves in life position in pre-Holocene sediments (cf. England et al., 2013). Instead, dateable material at the lowest stratigraphic level, assuming a deglacial contact below the level of core recovery, was chosen. In other cases, good materials for dating but in less ideal stratigraphic positions were chosen. Preferentially, filter feeders in pristine condition were primary targets, but due to limited availability some detritus feeders and/or fragmented shells were used. Cold water species of foraminifera were picked from the > 250 μm fraction for radiocarbon dating from cores JC106-016VC and JC106-18VC (hereafter denoted 16VC and 18VC, and similarly for other cores); picked species were predominantly *Cassidulina reniforme, Cassidulina neoteretis, Islandiella helenae, Islandiella norcrossi, Melonis barleeanus, Pullenia bulloides,* and *Triloculina tricarinata*. All samples were processed and AMS dated at the NERC Radiocarbon Laboratory, East Kilbride, UK. The ages have been calibrated using the Marine13 calibration curve (Reimer et al., 2013), with three selected reservoir ages ($\Delta R = 0$, $\Delta R = 300$ and $\Delta R = 700$ years; Table 3) as a sensitivity test of potential variability given known uncertainties regarding temporal and spatial variation in marine reservoir age in the North Atlantic during the last glacial cycle (Austin et al., 1995; Voelker et al., 2000; Waelbroeck et al., 2001; Peck et al., 2006; Singarayer et al., 2008). In relation to other uncertainties these different values for ΔR have a modest impact on the calibrated ages, so for the purposes of the discussion here ΔR is set to 0.

2.3. Micropalaeontology

Selected sections from three cores, 14VC, 18VC and 19VC (see panels F and G in Fig. 1), have been analysed for benthic foraminiferal assemblages in order to confirm the depositional context of specific facies and to highlight optimal horizons for radiocarbon dating. The samples were taken as slabs of the working half of the core sections; the outer edge was removed in order to avoid including smeared material. The 1 cm slabs were weighed and the volume determined using water displacement in a measuring cylinder. The samples for foraminifera analysis were sieved in tap water over a sieve set with mesh sizes of 63, 150, 500 μm and 1 mm. The residues were oven dried at 40 °C. Foraminifera were picked from the 150–500 μm size fraction. The > 150

Table 3
Radiocarbon determinations.

Sample identifier	Core	Publication code	Sample depth (cm)	Sample type	Conventional Radiocarbon Age (years BP)	+/− 1σ (radiocarbon yrs BP)	Calibrated Age (cal yrs BP) $R = 0$ years	+/− 2σ (cal yrs BP)	Calibrated Age (cal yrs BP) $R = 300$ years	+/− 2σ (cal yrs BP)	Calibrated Age (cal yrs BP) $R = 700$ years	+/− 2σ (cal yrs BP)
T4-007VC-313	JC106-007VC	SUERC-62448	313	shell fragment (sp?)	> 53,139				Infinite age			
T4-010VC-197	JC106-010VC	SUERC-62449	197	fragments (sp?)					Indistinguishable from background			
T4-010VC-279	JC106-010VC	SUERC-62450	279	broken shell (sp?)					Indistinguishable from background			
T4-012VC-62	JC106-012VC	SUERC-61838	62–63	articulated shell (*Nuculana pernula*)	23,272	81	27,233	216	26,889	323	26,374	274
T4-013VC-288	JC106-013VC	SUERC-58296	288–289	shell fragment (sp?)	55,394	2454			Infinite age			
T4-014VC-86	JC106-014VC	SUERC-62451	86	shell (*Macoma calcarea*)	20,747	57	24,423	227	24,105	206	23,665	231
T4-014VC-134	JC106-014VC	SUERC-58299	134–135	shell (*Macoma* cf. *moesta*)	20,860	54	24,601	294	24,220	206	23,787	220
T4-014VC-253	JC106-014VC	SUERC-62452	253	shell fragment (sp?)	22,765	66	26,648	329	26,263	233	25,923	141
T4-015VC-96	JC106-015VC	SUERC-58300	96–98	shell (Macoma cf. moesta)	21,109	56	24,955	321	24,515	272	24,066	206
T4-016VC-180	JC106-016VC	SUERC-66647	177–183	Cold water foraminifera (98 mg)	52,943	1836			Infinite age			
T4-018VC-137.5	JC106-018VC	SUERC-66648	137.5–140	Cold water foraminifera (298 mg)					Indistinguishable from background			
T4-018VC-177	JC106-018VC	SUERC-61842	177–178	shell fragment (Nuculana minuta?)					Indistinguishable from background			
T4-019VC-122	JC106-019VC	SUERC-58301	122–123	shell fragmentshell (sp?)					Indistinguishable from background			
T4-035VC-257	JC106-035VC	SUERC-61843	257	shell fragments (sp?)					Indistinguishable from background			
T4-041VC-59	JC106-041VC	SUERC-58302	59–60	shell (Macoma cf. moesta)	51,448	1502			Infinite age			
T4-044VC-68	JC106-044VC	SUERC-61844	68–70	shell fragments (Tellinidae)	57,896	3561			Infinite age			
T4-044VC-119	JC106-044VC	SUERC-58303	119–121	shell fragments (Tellinidae)	58,459	3586			Infinite age			
T4-045VC-67	JC106-045VC	SUERC-58304	67–69	shell fragments (Tellinidae)	20,713	66	24,383	231	24,070	218	23,626	247
T4-045VC-96	JC106-045VC	SUERC-61845	96–97	shell fragments (Tellinidae)	> 54,093				Infinite age			
T4-045VC-142	JC106-045VC	SUERC-58305	142–143	small shell fragments (sp?)	> 54,724				Infinite age			
T4-047VC-62	JC106-047VC	SUERC-62453	62.5	broken shell (sp?)	> 55,490				Infinite age			
T4-051PC-463	JC106-051PC	SUERC-58309	463	v small shell fragment (sp?)					Indistinguishable from background			
T4-052PC-389	JC106-052PC	SUERC-58306	389–390	intact shell (Mactra/Spisula sp)	9568	37	10,435	127	10,093	133	9517	76

μm fraction was selected because most shelf glacimarine forams are larger than deep Arctic species. The samples were split in a dry splitter; as many splits were analysed as was necessary for a count of at least 300 specimens of benthic foraminifera. Not all samples had sufficient foraminifera to make up a count of 300. Foraminifera concentrations were calculated as specimens per gram dry weight sediment. Foraminifera were identified to species level (where possible) according to Feyling-Hanssen et al. (1971). Additional sources used were Feyling-Hanssen and Buzas (1976) and Sejrup and Guilbault (1980).

The Fisher Alpha Diversity Index (α) was calculated using MATLAB and the formula $\alpha = N(1- x)/x$, where N is the number of specimens, and X is calculated iteratively using the eq. $S/N = (1-x)/x(-\ln(1-x))$, where S is the number of species. When the difference between S/N and X is ≤ 0.0001 the iteration is stopped.

3. Results

3.1. Sediment cores and facies description

A total of 51 cores were recovered in the Celtic Sea (Table 1). Lithostratigraphic logs of key cores are presented in Figs. 2–7; all remaining core logs are included in SI Fig. 1. Eight of the lithofacies described by Lockhart et al. (2018) are relevant to this study (notation based on Lockhart et al., 2018; Table 2).

The lithofacies logs indicate the distribution of these packages by core (Figs. 2–7). Lithofacies package LF10 (Fig. 2) was only recovered in core 3VC on the outer shelf at the southern extremity of Little Sole Bank (Fig. 1), where it is overlain by lithofacies package LF8 (Sm/Sl), LF2 (Gm) with an erosional basal contact to package LF8, and a thin veneer of package LF1 (Sm). A similar lithostratigraphy is observed in cores 14VC and 15VC which were recovered ~1.5 km apart on the outer shelf southeast of Cockburn Bank (Figs. 1 and 3), with lithofacies package LF8 (Sm/Sl/Sc with thin mud beds, Fm) overlain unconformably by packages LF2 (Gm) and LF1 (Sm). On the mid-shelf, LF8 occurs at the base of cores 18VC and 19VC which were recovered from topographic depressions between the linear sand ridges ~200 m apart (Figs. 1 and 5). Core 18VC contains basal muds corresponding to lithofacies package LF8 (Fm/Fl/Fp/Fd), with shear strengths of up to 110 kPa, unconformably overlain by packages LF2 (Gm) and LF1 (Fm). Facies corresponding to package LF8 in 19VC are much coarser, dominated by sands (Sm/Sl), with shear strengths of up to 150 kPa, but also some stratified (Fl) and massive muds (Fm). On the mid-shelf cores 33VC and 35VC were recovered ~ 336 m apart on the northwest flank of an unnamed bank northeast of Cockburn Bank (Figs. 1 and 4). The basal lithofacies package LF8 in core 33VC consists of deformed laminated muds (Fld), with shear strengths up to 133 kPa, unconformably overlain by massive gravels (Gm) fining upwards into lithofacies D (Sm, Fl). In core 35VC, basal lithofacies package LF8, consisting of massive (Sm) and stratified sand (Sl) and a thick laminated but not deformed bioturbated mud (Fl), with shear strengths of up to 148 kPa, is unconformably overlain by massive gravels (Gm) fining upwards into lithofacies LF1 (Sm, Fl). On the inner mid-shelf, cores 44VC and 45VC were recovered only 17 m apart on the northwest flank of Labadie Bank (Figs. 1 and 6). Both cores contain basal lithofacies LF9 package consisting of very coarse shelly sand, massive medium sand (Sm) overlain by laminated muds (Fl) of LF8 with shear strengths of up to 113 kPa for 44VC and 145 kPa for 45VC, and contorted laminated muds (Fld). On the inner shelf in the Celtic Deep, two piston cores, 51PC and 52PC were recovered (Figs. 1 and 7) penetrating four lithofacies LF1, LF1a, LF3 and LF4 consisting of basal massive (Fm) and laminated non-deformed muds (Fl) of lithofacies packages LF3 and LF4 overlain by a thin bed of LF1a and massive soft muds of lithofacies LF1.

PCA plots of the XRF data from the Celtic Sea cores indicate the close geochemical affinity of all LF8 and LF10 samples (Fig. 8). In particular, the diamict constituting LF10 from core 3VC is geochemically identical with LF8 from the other Celtic Sea cores.

3.2. Micropalaeontology

Lithofacies package LF8 has been analysed for benthic foraminifera from three cores, 14VC, 18VC and 19VC (Fig. 9). Core 14VC is dominated by *Elphidium excavatum* forma *clavata, Ammonia batavus, Lobatula lobatula* and *Quinqueloculina seminula* with associated *Cassidulina laevigata*, *Cassidulina reniforme* and *Islandiella helenae*. The latter species fluctuate with high (> 30% of the total benthic foraminiferal fauna) abundances between 3 and 2 m depth, a marked drop between 201 and 189 cm, and between 150 and 105 cm depth but with a spike at 96 cm depth. Species diversity is highest in the three uppermost samples. All samples also contain planktonic foraminifera with abundances up to 6%, with one exception (269, which only contains 29 foraminifera specimens).

Core 18VC is dominated by *I. helenae,* with associated *C. reniforme, E. excavatum* forma *clavata, Ammonia batavus* and *Bulimina marginata.* Core 19VC is dominated by *E. excavatum* forma *clavata, I. helenae* and *Haynesina germanica* with associated *C. reniforme* and *Haynesina orbiculare.* Abundances are rather similar throughout the core. Species diversity drops with decreasing depth; the samples below 1 m depth all have a Fisher's α of > 6, while above 82 cm α is < 6. Planktonic foraminifera were found in this core in abundances up to 8%, but with abundances dropping with decreasing depth.

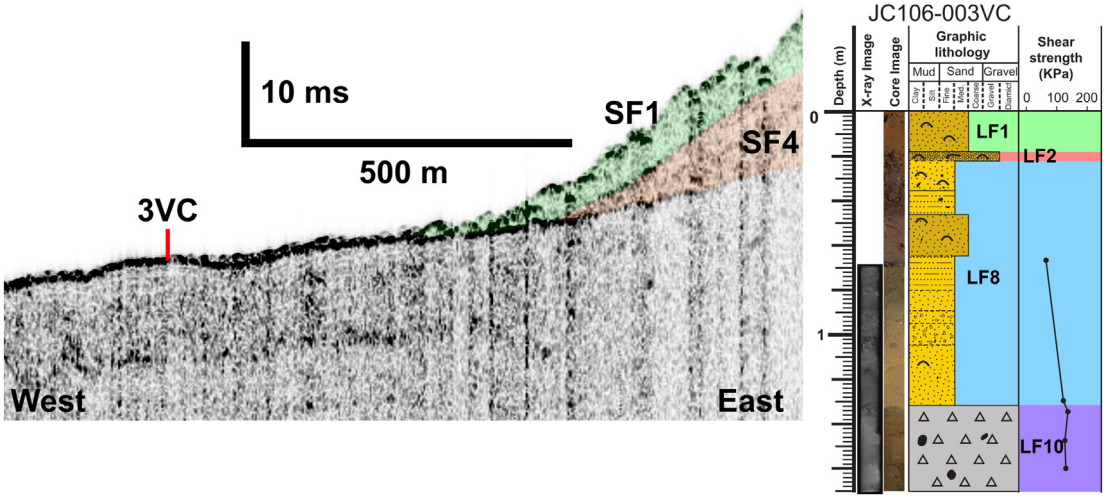

Fig. 2. Core 3VC: lithofacies log and seismic-stratigraphic context. See Fig. 1 Panel H for location.

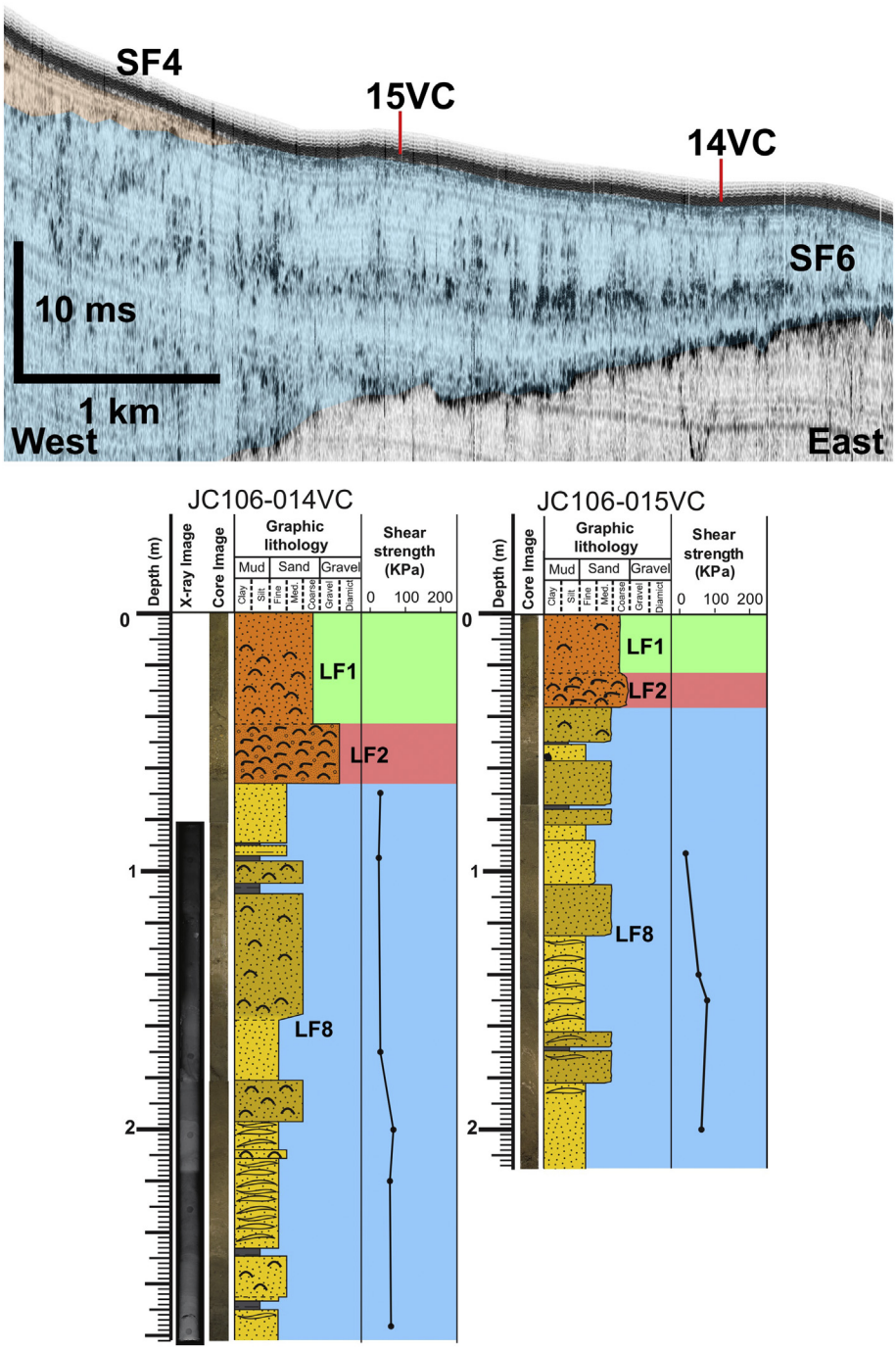

Fig. 3. Cores 14VC and 15VC: lithofacies log and seismic-stratigraphic context. See Fig. 1 Panel G for location.

3.3. Radiocarbon dating

Calcareous macro- and/or microfauna from sixteen of the cores from the Celtic Sea have been dated; six of these yielded finite ages, only one of which was post-glacial (Table 3). The full glacial ages were derived from cores 12VC, 14VC, 15VC, and 45VC, all from lithofacies package LF8. Cores 12VC, 14VC and 15VC are 4.7 km apart along the same transect of the flank of Cockburn Bank on the outer shelf (Fig. 1), in water depths of 65–170 m (Table 1) with dated materials from sand units within lithofacies LF8. The core 12VC radiocarbon determination is of 27.2 cal ka BP ($\Delta R = 0$) from a homogeneous stiff sand unit. Core 14VC 3 km to the northwest contains three full glacial ages; 26.6 cal ka BP at 253 cm to 24.4 cal ka BP ($\Delta R = 0$) at 86 cm from sandy facies which appear to be a lateral continuation of the sediments in core 12VC. Core 14VC can be correlated to core 15VC, 1.7 km to the northwest, which improves age control; the interval 246–156 cm in core 14VC corresponds to the interval 142–82 cm in core 15VC (Fig. 3), yielding a radiocarbon age of 25.0 cal ka BP ($\Delta R = 0$). This age corresponds to the expected age of the corresponding level in core 14VC. The radiocarbon age of 24.4 cal ka BP ($\Delta R = 0$) from core 45VC was taken from the top of a pebbly silt unit which corresponds to facies LF8 which comes close to seabed at the location of the core. The other 11 cores yielded infinite ages (Table 3).

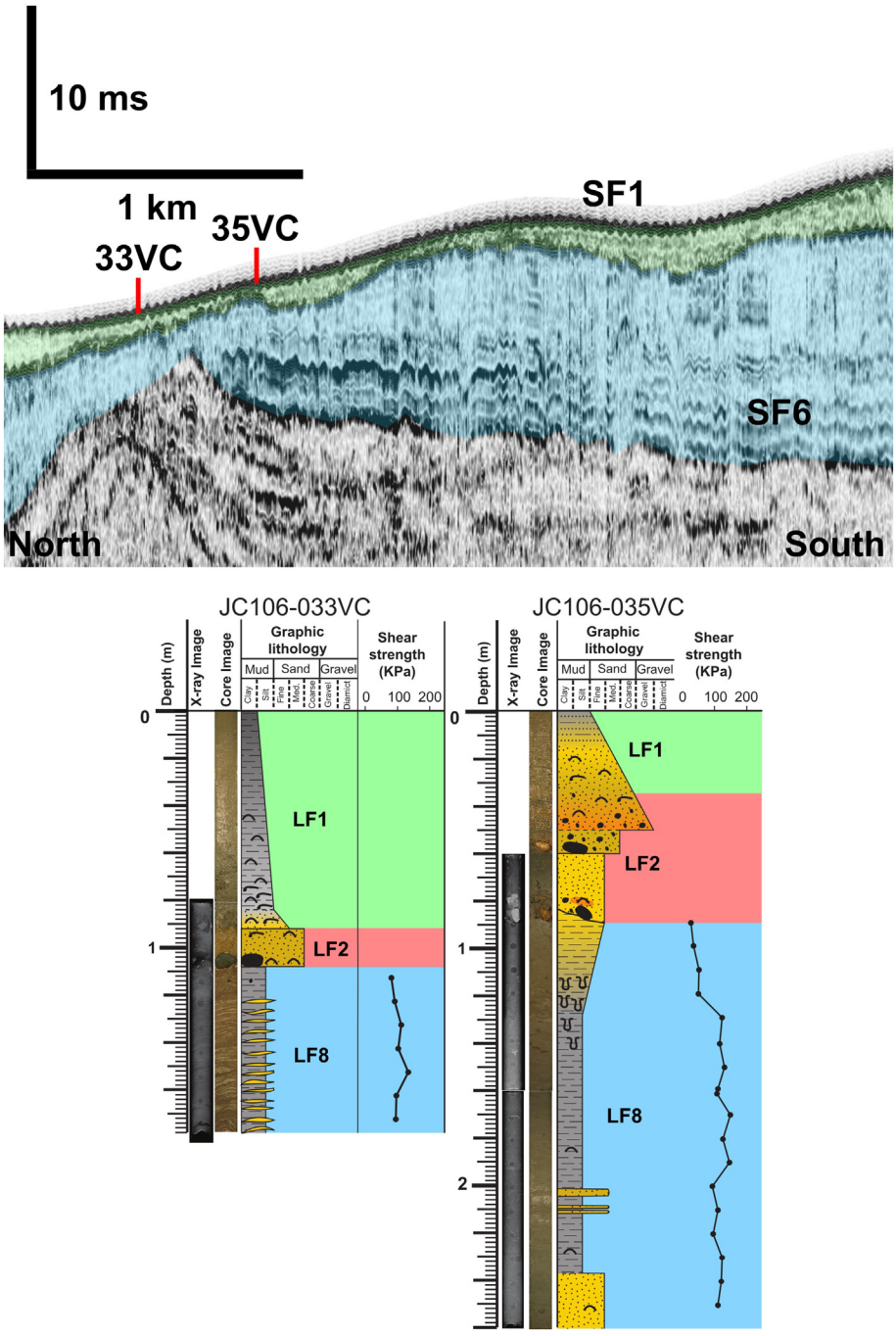

Fig. 4. Cores 33VC and 35VC: lithofacies log and seismic-stratigraphic context. See Fig. 1 Panel C for location.

4. Discussion

The sedimentary record represented by the lithofacies packages and correlative seismic facies across the Celtic shelf consist of facies that are interpreted to be of glacigenic (packages LF9, LF10, LF8, LF4 and LF3) and postglacial transgressive origin (packages LF2 and LF1). Post-glacial sediments correspond to shelf-side seafloor seismic facies SF1; on the mid- to outer shelf LF2 and LF1 correspond to an upward-fining succession (layers A and B of Pantin and Evans, 1984) consistent with decreasing energy conditions during progressive deepening of the shelf sea (Scourse et al., 2009b), while in the Celtic Deep they record persistent low energy deposition (Furze et al., 2014). The only diamicton recovered in any of the cores was from 3VC close to the shelf break, lithofacies LF10. The lithology of this matrix-supported unit strongly resembles the Melville Till described by Scourse et al. (1990) from the central Celtic Sea, and its overconsolidated character (shear strength of 127 kPa) is consistent with it being a subglacial till. At almost the same shelf break location clast-rich diamictons were previously cored and attributed by Scourse et al. (1990) to iceberg turbation. Iceberg turbation could be generated by grounded icebergs either from local ISIS sources or a far-field, possibly Laurentide, source; the latter suggestion is supported by the abundance of Laurentide-sourced IRD (Churchill Province) within Heinrich layer 2 in adjacent deep-sea cores (Scourse et al., 2009a; Haapaniemi et al., 2010). However, LF10 has a geochemical affinity identical with LF8 (Fig. 8) indicating that it is of ISIS origin. Another sample of clast-rich diamicton was described by Scourse et al. (1990) near outer Cockburn Bank, 20 km from the shelf edge and close to the site at which Praeg et al. (2015) recovered overconsolidated

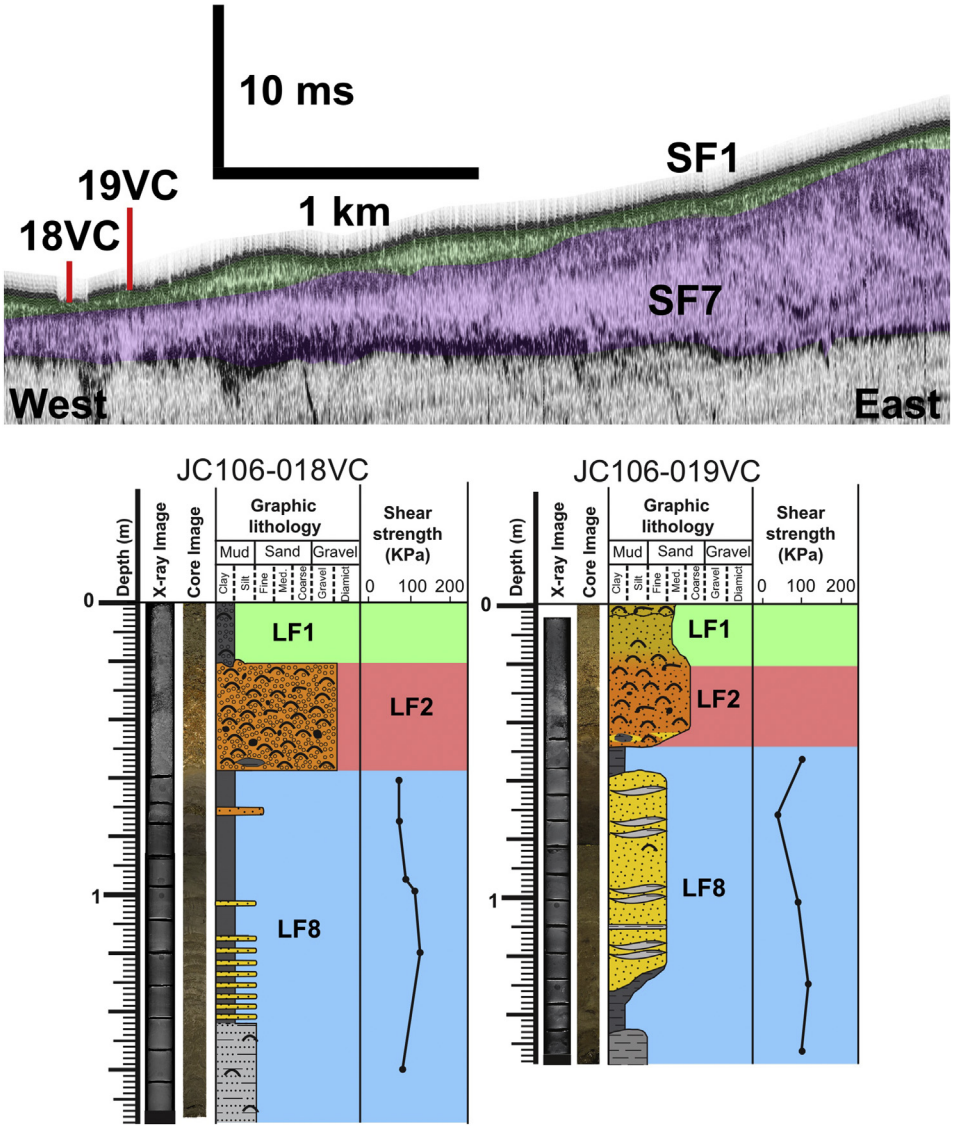

Fig. 5. Cores 18VC and 19VC: lithofacies log and seismic-stratigraphic context. See Fig. 1 Panel F for location.

stratified diamicts and glacimarine bedded muds. Here we interpret sediments acquired at the same site as deformed glacimarine sediments (lithofacies LF8, Fig. 3).

Lithofacies packages LF8 and LF9, distributed across the shelf, contain a wide variety of sand to mud facies, sometimes stratified, lensoid or laminated, very often contorted or deformed and with high shear strength. The foraminiferal assemblages from LF8 in cores 14VC, 18VC and 19VC contain a mixed cold- and warm-water assemblage. Cold water indicators, such as *C. laevigata*, *C. reniforme*, *I. helenae* and *E. excavatum* forma *clavata* (Mackensen and Hald, 1988; Steinsund, 1994; Hald and Korsun, 1997; Polyak et al., 2002; Jennings et al., 2004) occur alongside cold water bivalve molluscs such as *Macoma* and *Nuculana* spp. and thermophilous elements such as *A. batavus, L. lobatula* and *Q. seminula* (Murray, 1970; Mackensen and Hald, 1988; Walton and Sloan, 1990; Fig. 9). Such mixing of cold and warm elements is typical in the glacimarine sequences of the Irish Sea, where autochthonous cold water species are found alongside reworked allochthonous material entrained by the ice eroding older shallow water temperate sequences (Austin and McCarroll, 1992; Shakesby et al., 2000; Furze et al., 2014). This mixed assemblage is typical of the Melville Laminated Clay described by Scourse et al. (1990).

The mixing of in situ with reworked material explains the spread of radiocarbon ages deriving from this lithofacies package, older infinite ages coming from reworked material and finite ages from what we interpret as authochthonous material coeval with the deposition of LF8. These finite ages indicate, based on a reservoir age of $\Delta R = 0$, deposition between 27 and 24 ka BP. The sediments, structures and contained fauna of lithofacies package LF8 are all indicative of a glacimarine succession (Elverhøi et al., 1980; Andrews and Tedesco, 1992; Dowdeswell and Siegert, 1999) that can be correlated with the Melville Laminated Clay. It is possible that had the vibrocorer been able to penetrate further through the glacimarine sediments that further bodies of basal till would have been recovered (cf. Sejrup et al., 2005). One reason why penetration was limited (typically 1–2 m) is the extremely dense character, with high shear strengths, of many of the lithofacies package LF8 sediments; 115 kPa in 19VC, 125 kPa in 18VC, 133 kPa in 33VC and 148 kPa in 35VC. These sequences are also characterised by contorted and deformed structures typical of glacitectonism (cf. Lockhart et al., 2018). Similar characteristics were noted in the Melville Laminated Clay by Scourse et al. (1990) but attributed to the fact that the samples had significantly desiccated during storage prior to analysis. It is now evident that the density and shear strength of this material is a primary sedimentary characteristic, and not an artefact of curation. These facies are distributed as far as the shelf break. The

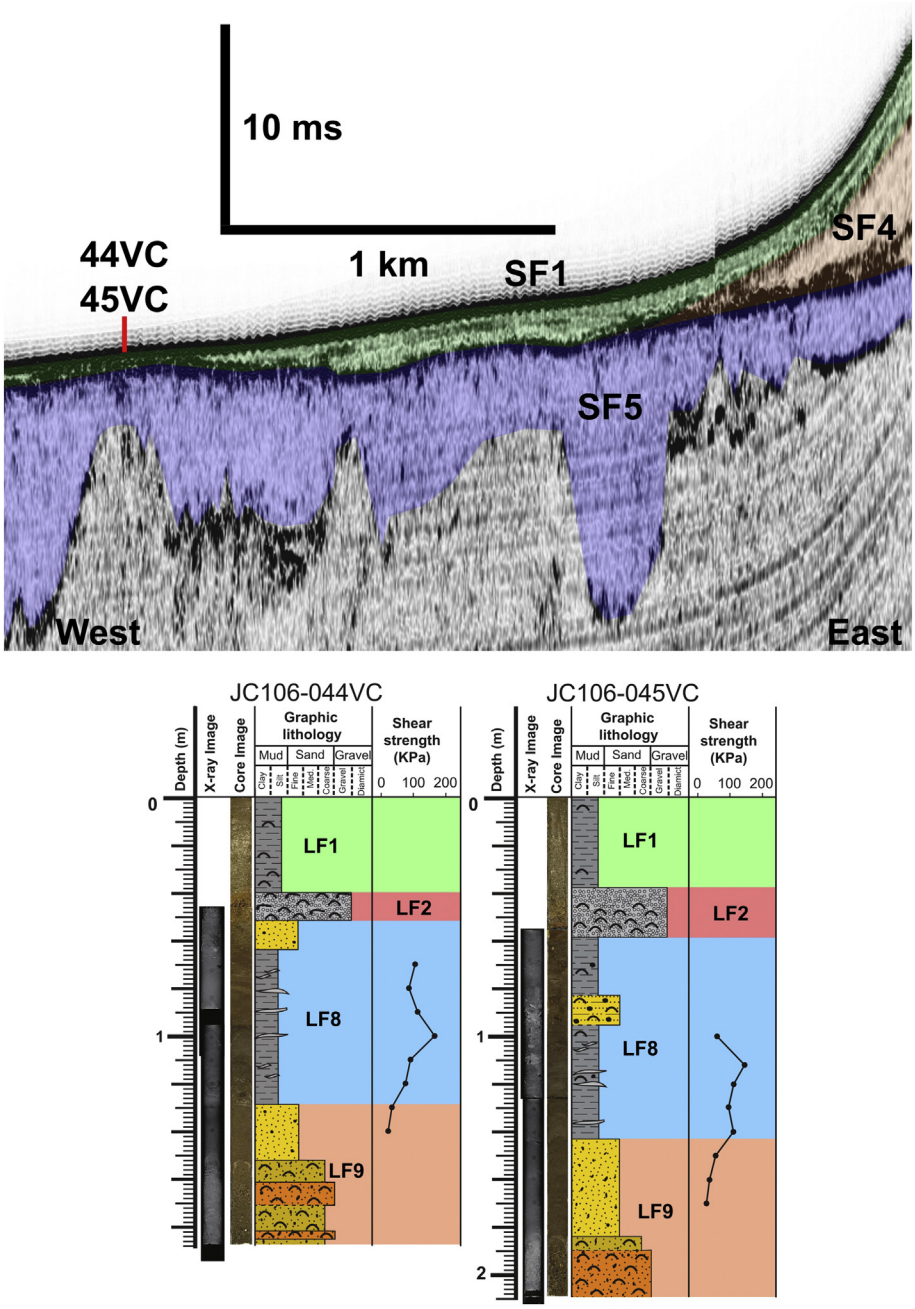

Fig. 6. Cores 44VC and 45VC: lithofacies log and seismic-stratigraphic context. See Fig. 1 Panel B for location.

demonstration that subglacial till underlies a glacitectonically deformed glacimarine sequence as far as the shelf break indicates that the deglacial sequence in the Celtic Sea cannot be accommodated within a simple and single advance-retreat model, but that initial retreat was followed by grounded ice readvance over previously deposited glacimarine material; it is not clear from the available evidence whether this was small- (~ < 1 km) or large-scale (up to 100 km) readvance of the ice terminus.

Not all the lithofacies package LF8 sequences were contorted; cores 2PC, 4-9VC (Fig. SI 1) penetrated soft, undeformed, glacimarine sequences with shear strength of ~40 kPa. Core 2PC (459 m water depth), recovered seaward of 3VC which contains basal diamict, we interpret not to have been overridden by ice, so constraining to ice limit between 2PC and 3VC. Cores 4-9VC were recovered shelfwards of 3VC and so probably within the ice limit. Lithofacies packages LF3 and LF4 from the Celtic Deep also consist of undeformed glacimarine massive and laminated muds, lateral equivalents of LF8. These show no sign of having been overridden by readvancing ice and indicate either relatively rapid retreat or deposition in deeper water.

The totality of the evidence supports the suggestion by Praeg et al. (2015) that ISIS extended as far as the Celtic shelf break in the Irish-UK sectors and was far more extensive than the mid-shelf limit proposed by Scourse et al. (1990) and Scourse and Furze (2001). Our results confirm the presence of glacigenic sediments at the site examined by Praeg et al. (2015), located 20 km from the shelf edge, and further provide evidence of subglacial and glacimarine sediments at the position of VC3, located at the shelf edge 100 km to the SW (Fig. 1). The distribution of till across the shelf and glacitectonised glacimarine sequences, and of undeformed glacimarine sediments, indicates the advance of the terminus of ISIS into the Celtic Sea as far as the Irish-UK sector of the shelf break. We have no evidence to test the possible advance of ice southeastwards into the French sector, though a change in the morphology of the linear

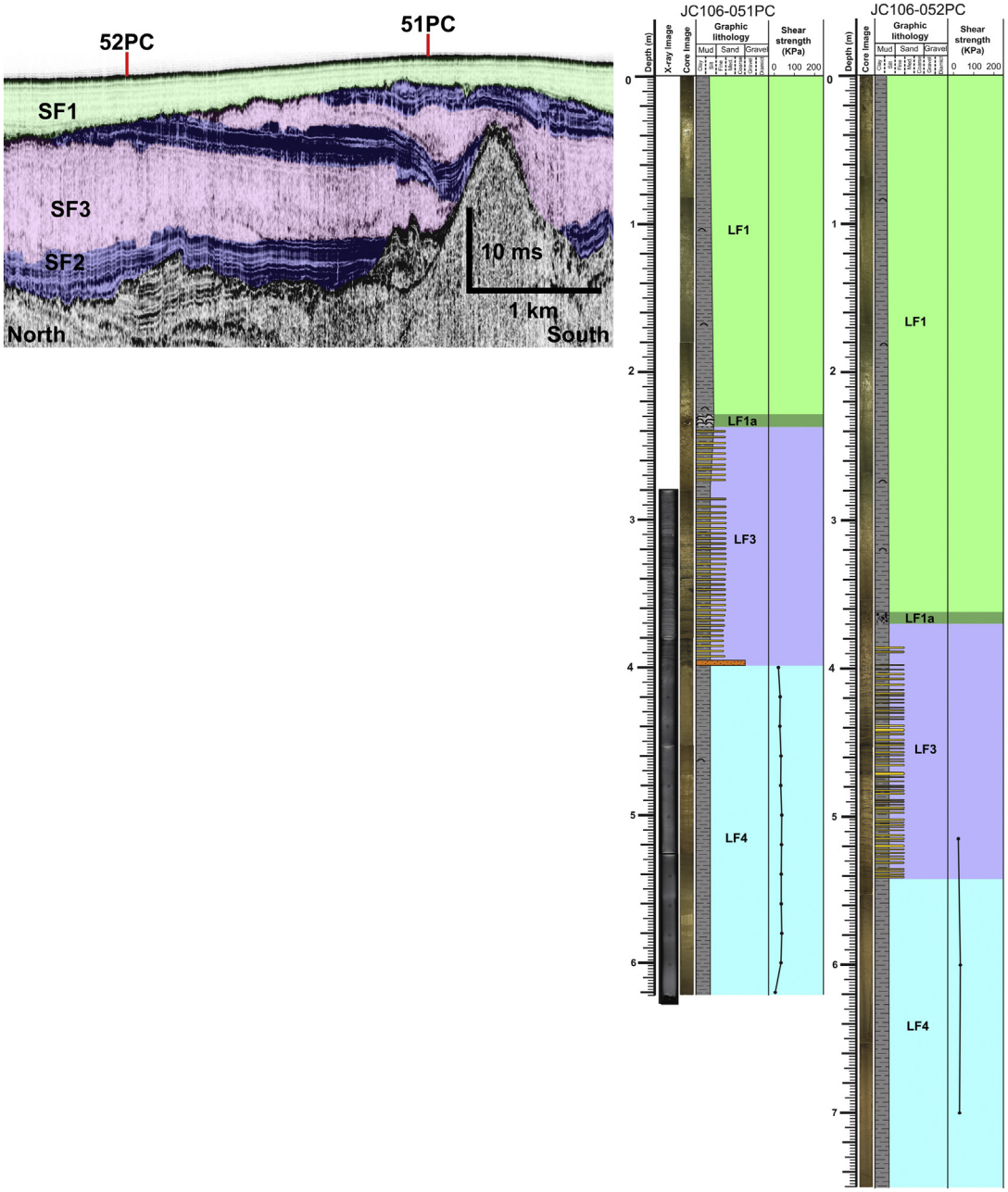

Fig. 7. Cores 51PC and 52PC: lithofacies log and seismic-stratigraphic context. See Fig. 1 Panel A for location.

sediment ridge field could suggest that this sector remained ice free (Lockhart et al., 2018). This suggestion remains to be tested.

The new radiocarbon data from lithofacies package LF8, indicating deposition between 27 and 24 cal ka BP, are consistent with the single determination published by Praeg et al. (2015) of 24.3 cal ka BP, and confirm the timing of the initial advance phase into the Celtic Sea. Geochronological analysis has recently been undertaken by BRITICE-CHRONO of the terrestrially-exposed retreat sequences along the ISIS retreat axis, in the Isles of Scilly using new combined optically-stimulated luminescence (OSL) and terrestrial cosmogenic nuclide (TCN) rock-exposure ages. Results indicate ISIS reached the islands at 25.5 ± 1.5 ka (Smedley et al., 2017b), slightly earlier than suggested by the legacy Bayesian analysis (Chiverrell et al., 2013) and the timing of the deep-sea Celtic Sea IRD signal (Haapaniemi et al., 2010) but consistent with the offshore ages presented here and by Praeg et al. (2015). The timing of the advance into the Celtic Sea is now tightly constrained by both offshore and onshore geochronological data. The distribution of facies offshore and the presence of a clear ice limit on Scilly (Scourse, 1991; Hiemstra et al., 2006) indicate that Scilly lay on the eastern lateral flank of the ISIS advance, and not in a terminal position.

The initial retreat of ISIS from the Celtic Sea was rapid. In eastern Ireland, new OSL and TCN data register the slowing of the retreat rate from 300 to 600 m yr^{-1} across the Celtic Sea to stabilisation (3 m a^{-1}) between 24.2 and 22.1 ka during Greenland Interstadial 2 in St George's Channel (Small et al., 2018). The timing of retreat indicated by a Bayesian analysis of the new eastern Irish data indicates the primacy of topographic and internal glaciological controls over external climatic (atmospheric and oceanographic) forcings in controlling ice stream behaviour within the axis of ISIS (Jamieson et al., 2012; Joughin et al., 2014; Mosola and Anderson, 2006; Small et al., 2018), but these controls cannot be responsible for the initiation of ice retreat from the shelf break at ~25 ka. However, the initiation of ice retreat from the continental shelf west of Ireland has also been dated to ~25 ka (Ó Cofaigh

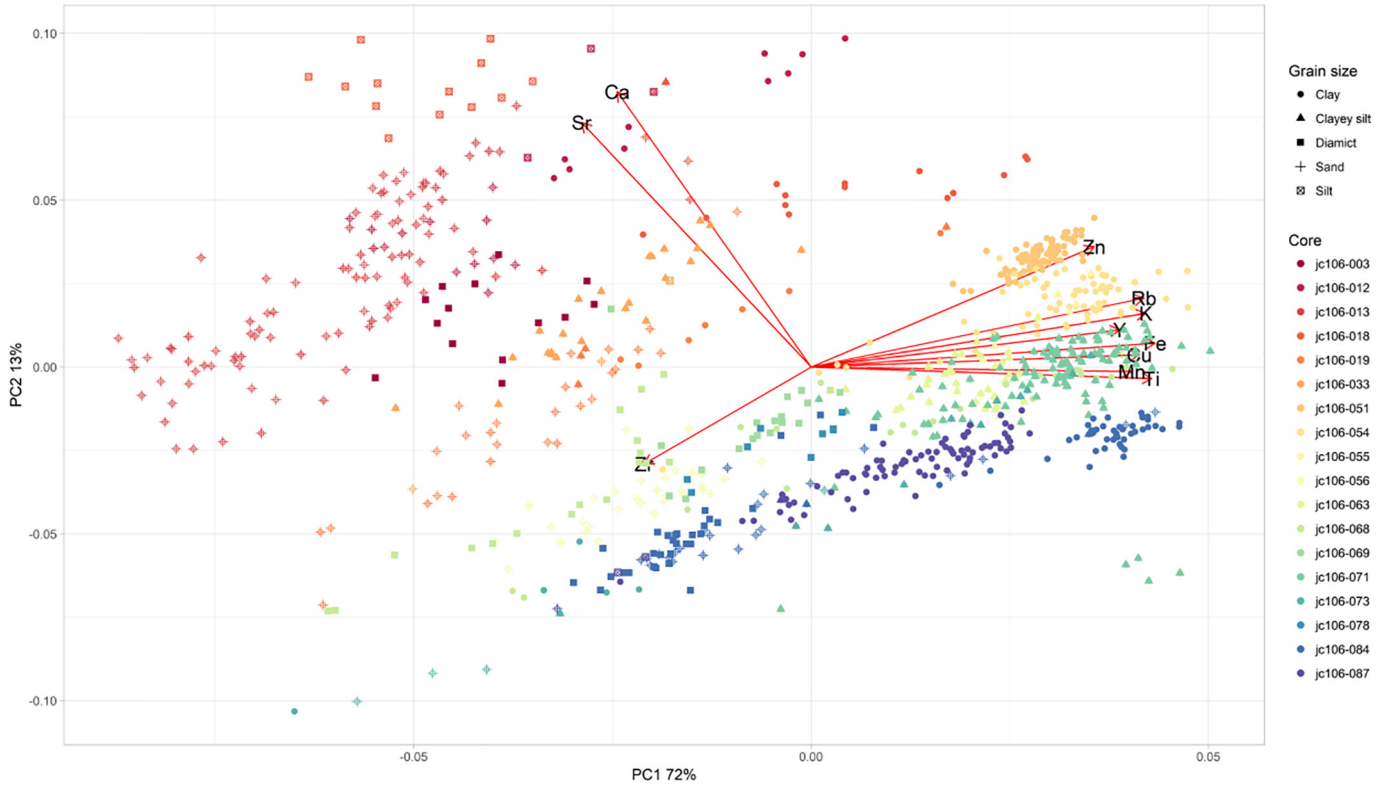

Fig. 8. PCA plot of LF8 and LF10 XRF data from Celtic and Irish Sea cores. Sediment grain size is indicated by symbol type (see legend) and colour denotes the different cores analysed. The distance between data points is a measure of the statistical similarity of samples in terms of their elemental geochemical characteristics. PC1 (x axis) explains 72% of the variance in the data and PC2 (y axis) explains 13% of the variance. The red lines indicate the elemental contributions to the PC axes; the main separation between individual cores results from changes in Ca and Sr content, and within cores by variability in the other elements analysed. Note that the diamict from core 3VC (JC106–003) plots within the field occupied by LF8 from other Celtic Sea cores. (For interpretation of the references to colour in this figure legend, the reader is referred to the web version of this article.)

et al., 2019). This synchrony may suggest deglaciation driven by rising/high relative sea level as a function of glacio-isostatic depression of the outer shelf during peak BIIS volume. If correct, this implies greater ice loads and glacio-isostatic depression over Britain and Ireland than hitherto considered likely (cf. Bradley et al., 2011). Palaeotidal simulations for the outer Celtic Sea (Ward et al., 2016) indicate high tidal amplitudes during full glacial conditions (Scourse et al., 2018) which would have accentuated deglaciation as a result of high relative sea level (Fig. 10). Available glacial isostatic adjustment simulations, which do not incorporate the revised ice extent and loads presented here, indicate falling relative sea level in the vicinity of St Georges Channel at 21 ka (Bradley et al., 2011) associated with very low tidal amplitudes (Ward et al., 2016; Fig. 10). Falling relative sea level combined with low tidal amplitudes likely decrease the rate of deglaciation and ice sheet retreat (Scourse et al., 2018) and these external factors may have combined with topographic and internal glaciological controls to determine the decrease in retreat rate as the ice front moved northwards out of the Celtic Sea into St George's Channel. The growth and decay phases of ISIS significantly precedes (by 3 ka) the other major ice stream in the system, the Norwegian Channel Ice Stream, most probably due to differences in the timing of ice sheet build up or that one or the other arises from internal glaciological instabilities.

While the existence of ISIS is well founded, its exact footprint remains ill-defined owing to few lateral geomorphological indicators such as a prominent edge to a field of mega-scale glacial lineations or shear margin moraines, and on the Celtic shelf there is a lack of obvious topography to constrain the margin. Nevertheless, a striking aspect is the large reconstructed width in comparison to other extant and palaeo ice streams from around the world. A width of the order of 100 km places ISIS at the wider end of the phenomena (Margold et al., 2015) and comparable to the Hudson Strait Ice Stream of the Laurentide Ice Sheet and the Thwaites Ice Stream in Antarctica. To maintain fast flow over such widths requires substantial feeder catchments that were probably unlikely from the BIIS. This suggests the ISIS could only exist as a transitory ice stream that rapidly drew down ice volumes. Our chronology of rapid advance and withdrawal is consistent with this, as are findings of numerical modelling investigations that struggle to simulate a steady state ice stream of this scale (Boulton and Hagdorn, 2006; Hubbard et al., 2009). It has also been a challenge for ice sheet models to simulate ice stream advance to the Isles of Scilly without building up ice elsewhere at locations more extensive than indicated by empirical evidence, such as mid and southern England (e.g. Patton et al., 2017). This problem is exacerbated by the Celtic Sea extent that we now report. Modelling investigations are underway to address this challenge.

5. Conclusions

Cored glacigenic sequences correlated to seismic stratigraphic units provide clear evidence of the advance and extent of the Irish Sea Ice Stream across the Celtic shelf during the Last Glacial. Overconsolidated subglacial diamicts (till) of ISIS origin have been recovered from close to the shelf break. Together with deformed and contorted proximal to distal glacimarine sequences containing distinctive cold water foraminiferal assemblages recovered from across the shelf, these diamicts indicate the advance of the ISIS into the Celtic Sea as far as the continental shelf break of the Irish and UK sectors of the Celtic Sea, and raises questions regarding the extent of ice into the French sector. The timing of this advance has been constrained by a series of new radiocarbon ages to between 27 and 24 cal ka BP. These ages are consistent with a single published radiocarbon determination from a glacimarine

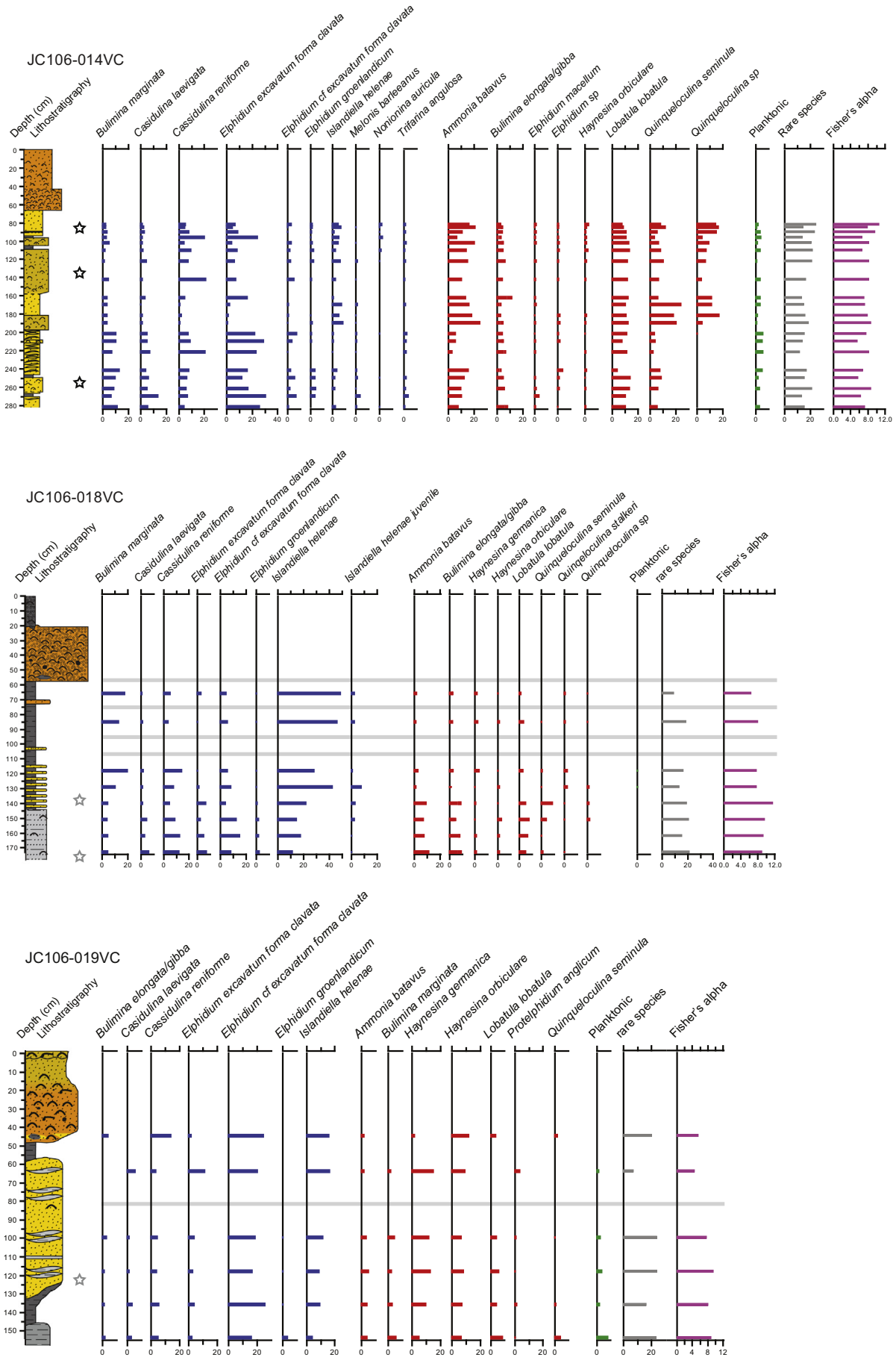

(caption on next page)

Fig. 9. Micropalaeontology of cores 14VC, 18VC and 19VC. Only species that comprise 5% of the total foraminiferal count in at least one sample are plotted. Other species are all included in 'rare species'. Grey lines: barren samples. Black stars: finite ^{14}C ages. Grey stars: ^{14}C dates on reworked shell material.

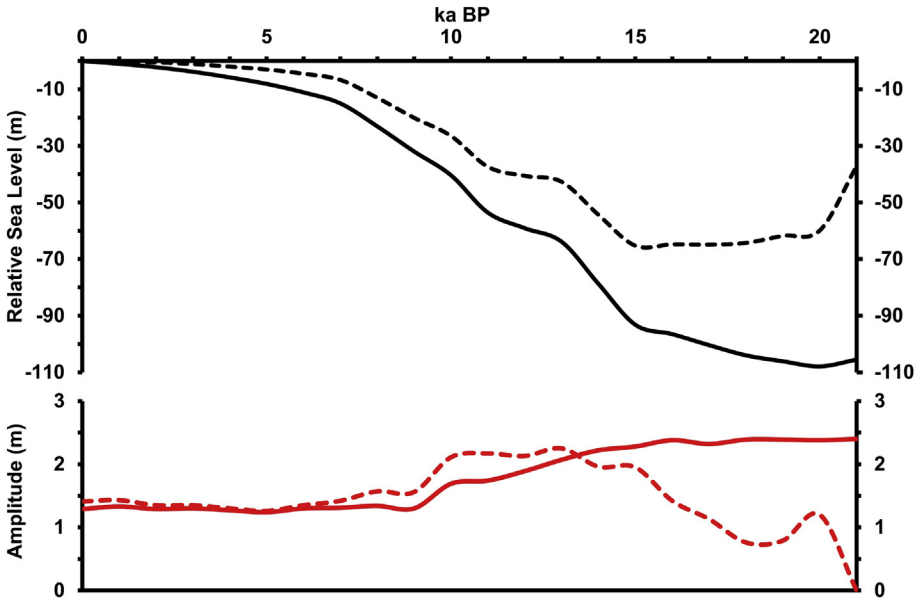

Fig. 10. Relative sea level (RSL) predictions for St. George's Channel (dashed) and the outer Celtic shelf (solid) based on GIA simulations (black; Bradley et al., 2011) with simulated tidal elevation amplitudes (red; Ward et al., 2016). See Fig. 1 for locations. (For interpretation of the references to colour in this figure legend, the reader is referred to the web version of this article.)

sequence recovered close to the shelf break, and with new geochronological data from the Isles of Scilly indicating ice advance at 25.5 ka. Comparison with ages for deglaciation farther north in the Irish Sea suggests that ice retreat across the Celtic shelf was initially rapid and then slowed, constrained by topographic controls, falling relative sea level and low tidal amplitudes in the vicinity of St George's Channel. Deglaciation on the outer shelf was probably initiated by high or rising sea level driven by glacio-isostatic depression during peak glaciation.

Supplementary data to this article can be found online at https://doi.org/10.1016/j.margeo.2019.03.003.

Acknowledgements

This research was funded by the UK Natural Environment Research Council Consortium Grant NE/J007196/1 'BRITICE-CHRONO'. The work was supported by the NERC Radiocarbon Facility (allocations1530.0311, 1577.0911 and 1606.0312). We thank the staff at the SUERC AMS Laboratory, East Kilbride for carbon isotope measurements, and the crews of the RRS *James Cook*, the BGS vibrocorer and the NOC piston corer. Daniel Praeg's participation has been in part supported by the Italian PNRA project IPY GLAMAR (grant number 2009/A2.15). We thank Dr. Jenna Tugwell, research radiographer at Ysbyty Gwynedd, for producing the X-ray images. We thank Dr. Mark Furze and Dr. Graham Oliver for help with bivalve identification, and Dr. Sarah Bradley for discussion on glacial-isostatic adjustment simulations. Two anonymous referees are acknowledged for their comments that helped to improve the manuscript significantly.

References

Andrews, J.T., Tedesco, K., 1992. Detrital carbonate-rich sediments, northwestern Labrador Sea: Implications for ice-sheet dynamics and iceberg rafting (Heinrich) events in the North Atlantic. Geology 20, 1087–1090.

Austin, W.E.N., McCarroll, D., 1992. Foraminifera from the Irish Sea glacigenic deposits at Aberdaron, western Lleyn, North Wales: palaeoenvironmental implications. J. Quat. Sci. 7, 311–317.

Austin, W.E.N., Bard, E., Hunt, J.B., Kroon, D., Peacock, J.D., 1995. The ^{14}C age of the Icelandic Vedde Ash: implications for Younger Dryas marine reservoir age corrections. Radiocarbon 37, 53–62.

Belderson, R.H., Pingree, R.D., Griffiths, D.K., 1986. Low sea-level tidal origin of Celtic Sea sand banks — evidence from numerical modelling of M2 tidal streams. Mar. Geol. 73, 99–108.

Boulton, G., Hagdorn, M., 2006. Glaciology of the British Isles Ice Sheet during the last glacial cycle: form, flow, streams and lobes. Quat. Sci. Rev. 25, 3359–3390.

Boyle, J.F., Chiverrell, R.C., Schillereff, D., 2015. Approaches to water content correction and calibration for μXRF core scanning: comparing X-ray scattering with simple regression of elemental concentrations. In: Croudace, I.W., Rothwell, R.G. (Eds.), Micro-XRF Studies of Sediment Cores. Springer, Netherlands, pp. 373–390.

Bradley, S.L., Milne, G.A., Shennan, I., Edwards, R., 2011. An improved glacial isostatic adjustment model for the British Isles. J. Quat. Sci. 26, 541–552.

Chiverrell, R.C., Thrasher, I.M., Thomas, G.S., Lang, A., Scourse, J.D., van Landeghem, K.J., Mccarroll, D., Clark, C.D., Cofaigh, C.Ó., Evans, D.J., Ballantyne, C.K., 2013. Bayesian modelling the retreat of the Irish Sea Ice Stream. J. Quat. Sci. 28, 200–209.

Chiverrell, R.C., Smedley, R.K., Small, D., Callantyne, C.K., Burke, M.J., Callard, S.L., Clark, C.D., Duller, G.A.T., Evans, D.J.A., Van Landeghem, K., Livingstone, S., Ó Cofaigh, C., Thomas, G.S.P., Roberts, D.H., Saher, M., Scourse, J.D., Wilson, P., 2018. Ice margin oscillations during deglaciation of the northern Irish Sea Basin. J. Quat. Sci. 33, 739–762.

Clark, C.D., Hughes, A.L., Greenwood, S.L., Jordan, C., Sejrup, H.P., 2012. Pattern and timing of retreat of the last British-Irish Ice Sheet. Quat. Sci. Rev. 44, 112–146.

Clark, C.D., Ely, J.C., Greenwood, S.L., Hughes, A.L.C., Meehan, R., Barr, I.D., Bateman, M.D., Bradwell, T., Doole, J., Evans, D.J.A., Jordan, C.J., Monteys, X., Pellicer, X.M., Sheehy, M., 2018. BRITICE glacial map, version 2: a map and GIS database of glacial landforms of the last British–Irish Ice Sheet. Boreas 47, 11–28.

Dowdeswell, J.A., Siegert, M.J., 1999. Ice-sheet numerical modeling and marine geophysical measurement of glacier-derived sedimentation on the Eurasian continental margins. Geol. Soc. Am. Bull. 111, 1080–1097.

Elverhøi, A., Liestøl, O., Nagy, J., 1980. Glacial erosion, sedimentation and microfauna in the inner part of Kongsfjorden, Spitsbergen. Nor. Polarinst. Skr. 172, 33–58.

England, J., Dyke, A.S., Coulthard, R.D., Mcneely, R., Aitken, A., 2013. The exaggerated radiocarbon age of deposit-feeding molluscs in calcareous environments. Boreas 42, 362–373.

Feyling-Hanssen, R.W., Buzas, M.A., 1976. Emendation of *Cassidulina* and *Islandiella helenae* new species. J. Foraminifer. Res. 6, 154–158.

Feyling-Hanssen, R.W., Jørgensen, J.A., Knudsen, K.L., Lykke-Andersen, A.L., 1971. Late quaternary foraminifera from Vendsyssel, Denmark and Sandnes, Norway. Bull. Geol. Soc. Den. 21, 67–317.

Furze, M.F., Scourse, J.D., Pieńkowski, A.J., Marret, F., Hobbs, W.O., Carter, R.A., Long, B.T., 2014. Deglacial to postglacial palaeoenvironments of the Celtic Sea: lacustrine conditions versus a continuous marine sequence. Boreas 43, 149–174.

Haapaniemi, A.I., Scourse, J.D., Peck, V.L., Kennedy, H., Kennedy, P., Hemming, S.R., Furze, M.F., Pieńkowski, A.J., Austin, W.E., Walden, J., Wadsworth, E., 2010. Source, timing, frequency and flux of ice-rafted detritus to the Northeast Atlantic margin, 30–12 ka: testing the Heinrich precursor hypothesis. Boreas 39, 576–591.

Hald, M., Korsun, S., 1997. Distribution of modern benthic foraminifera from fjords of Svalbard, European Arctic. J. Foraminifer. Res. 27, 101–122.

Hiemstra, J.F., Evans, D.J.A., Scourse, J.D., McCarroll, D., Furze, M.F.A., Rhodes, E., 2006. New evidence for a grounded Irish Sea glaciation of the Isles of Scilly, UK. Quat. Sci. Rev. 25, 299–309.

Hubbard, A., Bradwell, T., Golledge, N., Hall, A., Patton, H., Sugden, D., Cooper, R., Stoker, M., 2009. Dynamic cycles, ice streams and their impact on the extent, chronology and deglaciation of the British-Irish Ice Sheet. Quat. Sci. Rev. 28,

758–776.
Jamieson, S.S., Vieli, A., Livingstone, S.J., Cofaigh, C.Ó., Stokes, C., Hillenbrand, C.D., Dowdeswell, J.A., 2012. Ice-stream stability on a reverse bed slope. Nat. Geosci. 5, 799–802.
Jennings, A.E., Weiner, N.J., Helgadottir, G., Andrews, J.T., 2004. Modern foraminiferal faunas of the southwestern to northern Iceland Shelf; oceanographic and environmental controls. J. Foraminifer. Res. 34 (3), 180–207.
Joughin, I., Alley, R.B., 2011. Stability of the West Antarctic ice sheet in a warming world. Nat. Geosci. 4, 506–513.
Joughin, I., Smith, B.E., Medley, B., 2014. Marine ice sheet collapse potentially under way for the Thwaites Glacier Basin, West Antarctica. Science 344, 735–738.
Lockhart, E.A., Scourse, J.D., Praeg, D., Van Landeghem, K.J.J., Mellett, C., Saher, M., Callard, L., Chiverrell, R.C., Benetti, S., O'Cofaigh, C., Clark, C.D., 2018. A stratigraphic investigation of the Celtic Sea megaridges based on seismic and core data from the Irish-UK sectors. Quat. Sci. Rev. 198, 156–170.
Mackensen, A., Hald, M., 1988. *Cassidulina teretis* Tappan and *C. laevigata* d'Orbigny; their modern and late Quaternary distribution in northern seas. J. Foraminifer. Res. 18, 16–24.
Margold, M., Stokes, C.R., Clark, C.D., 2015. Ice streams in the Laurentide Ice Sheet: identification, characteristics and comparison to modern ice sheets. Earth Sci. Rev. 143, 117–146.
McCarroll, D., Stone, J.O., Ballantyne, C.K., Scourse, J.D., Fifield, L.K., Evans, D.J., Hiemstra, J.F., 2010. Exposure-age constraints on the extent, timing and rate of retreat of the last Irish Sea ice stream. Quat. Sci. Rev. 29, 1844–1852.
Mosola, A.B., Anderson, J.B., 2006. Expansion and rapid retreat of the West Antarctic Ice Sheet in eastern Ross Sea: possible consequence of over-extended ice streams? Quat. Sci. Rev. 25, 2177–2196.
Murray, J.W., 1970. Foraminifers of the western approaches to the English Channel. Micropaleontology 16, 471–485.
Ó Cofaigh, C., Evans, D.J., 2007. Radiocarbon constraints on the age of the maximum advance of the British–Irish Ice Sheet in the Celtic Sea. Quat. Sci. Rev. 26, 1197–1203.
Ó Cofaigh, C., Telfer, M.W., Bailey, R.M., Evans, D.J., 2012. Late Pleistocene chronostratigraphy and ice sheet limits, southern Ireland. Quat. Sci. Rev. 44, 160–179.
Ó Cofaigh, C., Weilbach, K., Lloyd, J.M., Benetti, S., Callard, L., Purcell, C., Civerrell, R.C., Dunlop, P., Saher, M., Livingstone, S.J., Van Landeghem, K.J.J., Moreton, S.G., Clark, C.D., Fabel, D., 2019. Early deglaciation of the British-Irish Ice Sheet on the Atlantic shelf northwest of Ireland driven by glacioisostatic depression and high relative sea level. Quat. Sci. Rev. 208, 76–96.
Pantin, H.M., Evans, C.D.R., 1984. The Quaternary history of the central and southwestern Celtic Sea. Mar. Geol. 57, 259–293.
Patton, H., Hubbard, A., Andreassen, K., Auriac, A., Whitehouse, P.L., Stroeven, A.P., Shackleton, C., Winsborrow, M., Heyman, J., Hall, A.M., 2017. Deglaciation of the Eurasian ice sheet complex. Quat. Sci. Rev. 169, 148–172.
Peck, V.L., Hall, I.R., Zahn, R., Elderfield, H., Grousset, F., Hemming, S.R., Scourse, J.D., 2006. High resolution evidence for linkages between NW European ice sheet instability and Atlantic meridional overturning circulation. Earth Planet. Sci. Lett. 243, 476–488.
Polyak, L., Korsun, S., Febo, L.A., Stanovoy, V., Khusid, T., Hald, M., Paulsen, B.E., Lubinski, D.J., 2002. Benthic foraminiferal assemblages from the southern Kara Sea, a river-influenced arctic marine environment. J. Foraminifer. Res. 32, 252–273.
Praeg, D., McCarron, S., Dove, D., Cofaigh, C.Ó., Scott, G., Monteys, X., Facchin, L., Romeo, R., Coxon, P., 2015. Ice sheet extension to the Celtic Sea shelf edge at the last Glacial Maximum. Quat. Sci. Rev. 111, 107–112.
Reimer, P.J., Bard, E., Bayliss, A., Beck, J.W., Blackwell, P.G., Ramsey, C.B., Buck, C.E., Cheng, H., Edwards, R.L., Freidrich, M., Grootes, P.M., Guilderson, T.P., Haflidason, H., Hajdas, I., Hatte, C., Heaton, T.J., Hoffmann, D.L., Hogg, A.G., Hughen, K.A., Kaiser, K.F., Kromer, B., Manning, S.W., Niu, M., Reimer, R.W., Richards, D.A., Scott, E.M., Southon, J.R., Staff, R.A., Turney, C.S.M., van der Plicht, J., 2013. INTCAL and MARINE 13 radiocarbon age calibration curves 0-50,000 years cal BP. Radiocarbon 55, 1869–1887.
Rignot, E., Mouginot, J., Morlighem, M., Seroussi, H., Scheuchl, B., 2014. Widespread, rapid grounding line retreat of Pine Island, Thwaites, Smith, and Kohler glaciers, West Antarctica, from 1992 to 2011. Geophys. Res. Lett. 41, 3502–3509.
Roberts, D.H., Dackombe, R.V., Thomas, G.S., 2007. Palaeo-ice streaming in the central sector of the British—Irish Ice Sheet during the Last Glacial Maximum: evidence from the northern Irish Sea Basin. Boreas 36, 115–129.
Schoof, C., 2007. Ice sheet grounding line dynamics: Steady states, stability, and hysteresis. J. Geophys. Res. Earth Surf. 112 (F3) (article F000664).
Scourse, J.D., 1991. Late Pleistocene stratigraphy and palaeobotany of the Isles of Scilly. Philos. Trans. R. Soc. Lond. B334, 405–448.
Scourse, J.D., Furze, M.F.A., 2001. A critical review of the glaciomarine model for Irish Sea deglaciation: evidence from southern Britain, the Celtic shelf and adjacent continental slope. J. Quat. Sci. 16, 419–434.
Scourse, J.D., Austin, W.E.N., Bateman, R.M., Catt, J.A., Evans, C.D.R., Robinson, J.E., Young, J.R., 1990. Sedimentology and micropalaeontology of glacimarine sediments from the central and southwestern Celtic Sea. Geol. Soc. Lond., Spec. Publ. 53, 329–347.
Scourse, J.D., Robinson, E., Evans, C.D.R., 1991. Glaciation of the central and southwestern Celtic Sea. In: Glacial Deposits in Great Britain and Ireland. Balkema, Rotterdam, pp. 301–310.
Scourse, J.D., Haapaniemi, A.I., Colmenero-Hidalgo, E., Peck, V.L., Hall, I.R., Austin, W.E., Knutz, P.C., Zahn, R., 2009a. Growth, dynamics and deglaciation of the last British–Irish ice sheet: the deep-sea ice-rafted detritus record. Quat. Sci. Rev. 28, 3066–3084.
Scourse, J., Uehara, K., Wainwright, A., 2009b. Celtic Sea linear tidal sand ridges, the Irish Sea Ice Stream and the Fleuve Manche: palaeotidal modelling of a transitional passive margin depositional system. Mar. Geol. 259, 102–111.
Scourse, J.D., Ward, S.L., Wainwright, A., Uehara, K., Bradley, S., 2018. The role of megatides and relative sea level in controlling the deglaciation of the British-Irish and Fennoscandian Ice Sheets. J. Quat. Sci. 33, 139–149.
Sejrup, H.P., Guilbault, J.P., 1980. Cassidulina reniforme and C. obtuse (Foraminifera), taxonomy, distribution, and ecology. Sarsia 65, 79–85.
Sejrup, H.P., Hjelstuen, B.O., Dahlgren, K.T., Haflidason, H., Kuijpers, A., Nygård, A., Praeg, D., Stoker, M.S., Vorren, T.O., 2005. Pleistocene glacial history of the NW European continental margin. Mar. Pet. Geol. 22, 1111–1129.
Shakesby, R.A., Austin, W.E.N., McCarroll, D., 2000. Foraminifera from the glacigenic deposits at Broughton Bay, South Wales: a further test of the glaciomarine model of deglaciation of the Irish Sea. Proc. Geol. Assoc. 111, 147–152.
Singarayer, J.S., Richards, D.A., Ridgwell, A., Valdes, P.J., Austin, W.E.N., Beck, J.W., 2008. An oceanic origin for the increase of atmospheric radiocarbon during the Younger Dryas. Geophys. Res. Lett. 35, L14707.
Small, D., Smedley, R.K., Chiverrell, R.C., Scourse, J.D., Ó Cofaigh, C., Duller, G.A.T., McCarron, S., Burke, M.J., Evans, D.J.A., Fabel, D., Gheorghiu, D.M., Thomas, G.S.P., Xu, S., Clark, C.D., 2018. Trough geometry was a greater influence than climate-ocean forcing in regulating retreat of the marine-based Irish-Sea Ice Stream. Geol. Soc. Am. Bull. https://doi.org/10.1130/B31852.1.
Smedley, R.K., Chiverrell, R.C., Ballantyne, C.K., Burke, M.J., Clark, C.D., Duller, G.A.T., Fabel, D., McCarroll, D., Scourse, J.D., Small, D., Thomas, G.S.P., 2017a. Internal dynamics condition centennial-scale oscillations in marine-based ice-stream retreat. Geol. Soc. Am. Bull. 45, 787–790.
Smedley, R.K., Scourse, J.D., Small, D., Hiemstra, J.F., Duller, G.A.T., Bateman, M.D., Burke, M.J., Chiverrell, R.C., Clark, C.D., Davies, S.M., Fabel, D., 2017b. New age constraints for the limit of the British–Irish Ice Sheet on the Isles of Scilly. J. Quat. Sci. 32, 48–62.
Steinsund, P.I., 1994. Benthic Foraminifera in Surface Sediments of the Barents and Kara Seas: Modern and Late Quaternary Applications. University of Tromsø, Tromsø (111 pp).
Stokes, C.R., Tarasov, L., Blomdin, R., Cronin, T.M., Fisher, T.G., Gyllencreutz, R., Hättestrand, C., Heyman, J., Hindmarsh, R.C., Hughes, A.L., Jakobsson, M., 2015. On the reconstruction of palaeo-ice sheets: recent advances and future challenges. Quat. Sci. Rev. 125, 15–49.
Voelker, A., Grootes, P.M., Nadeau, M.J., Sarnthein, M., 2000. Radiocarbon levels in the Iceland Sea from 25–53 kyr and their link to the earth's magnetic field intensity. Radiocarbon 42, 437–452.
Waelbroeck, C., Duplessy, J.C., Michel, E., Labeyrie, L., Paillard, D., Duprat, J., 2001. The timing of the last deglaciation in the North Atlantic climate records. Nature 412, 724–727.
Walton, W.R., Sloan, B.J., 1990. The genus *Ammonia* Bruennich, 1772; its geographic distribution and morphologic variability. J. Foraminifer. Res. 20, 128–156.
Ward, S.L., Neill, S.P., Scourse, J.D., Bradley, S., Uehara, K., 2016. Sensitivity of palaeotidal models of the northwest European shelf seas to Glacial Isostatic Adjustment since the Last Glacial Maximum. Quat. Sci. Rev. 151, 198–211.